C. R. Chimie 14 (2011) 896–903

Contents lists available at ScienceDirect

Comptes Rendus Chimie

www.sciencedirect.com

Full paper/Mémoire

Mechanochemical synthesis of strontium britholites: Reaction mechanism

Nadia Gmati [a], Khaled Boughzala [a], Mohieddine Abdellaoui [b], Khaled Bouzouita [a,*]

[a] UR matériaux inorganiques, institut préparatoire aux études d'ingénieur de Monastir, University of Monastir, 5000 Monastir, Tunisia
[b] Laboratoire des matériaux utiles, INRAP, Technopole Sidi Thabet, 2020 Sidi Thabet, Tunisia

ARTICLE INFO

Article history:
Received 26 January 2011
Accepted after revision 27 April 2011
Available online 8 June 2011

Keywords:
Britholite
Strontium
Lanthanum
Mechanochemical synthesis
Reaction mechanism

ABSTRACT

The britholites have gained a great interest thanks to their potential applications as matrices for the confinement of the byproducts in the nuclear industry such as minor actinides and long-lived fission products. However, the preparation of britholites requires high temperatures, above 1200 °C. In this work, we strive to prepare these kinds of compounds by a mechanochemical synthesis at room temperature from the starting materials SrF_2, $SrCO_3$, $Sr_2P_2O_7$, La_2O_3 and SiO_2 using a planetary ball mill. The obtained results showed that the prepared products were carbonated apatites and the corresponding powders contained some unreacted silica and lanthana. To obtain pure britholites, a heat-treatment at 1100 °C was required. The mechanism involved in the different steps of the reaction is discussed in this paper. The obtained results suggest that the use of raw materials containing no carbonate is expected to directly lead to pure britholites by appropriate milling at room temperature.

© 2011 Académie des sciences. Published by Elsevier Masson SAS. All rights reserved.

RÉSUMÉ

Les britholites ont acquis un grand intérêt ces dernières années en raison de leur application potentielle comme matrices pour le confinement des déchets nucléaires, tels que les actinides mineurs et les produits de fission. Cependant, leur synthèse nécessite des températures élevées, supérieures à 1200 °C. L'objectif de ce travail est de préparer ces composés par mécanosynthèse à température ambiante, en utilisant SrF_2, $SrCO_3$, $Sr_2P_2O_7$, La_2O_3 et SiO_2 comme réactifs. Les résultats obtenus montrent que les produits préparés sont des apatites carbonatées et que certaines quantités de SiO_2 et La_2O_3 n'ont pas participé à la réaction. L'obtention de britholites pures a nécessité un traitement thermique à 1100 °C. Les mécanismes impliqués dans les différentes étapes de la réaction ont aussi été discutés. L'ensemble des résultats donne à penser que l'utilisation de réactifs ne contenant pas de carbonate devrait conduire à la formation de britholites pures par un broyage approprié à température ambiante.

© 2011 Académie des sciences. Publié par Elsevier Masson SAS. Tous droits réservés.

1. Introduction

Britholites, which are phosphosilicated apatites, are the subject of numerous studies both at the fundamental and the experimental levels. Since the discovery of the Oklo site [1,2], they have been considered to be particularly promising for use as matrices for the confinement of nuclear waste [3–9]. Indeed, this discovery showed that these materials can retain fission products over several million years without suffering damage [10]. Furthermore, several studies have shown that these compounds present a good resistance to aqueous alteration [11–14] and irradiation [15,16].

* Corresponding author.
E-mail address: khaled.bouzouita@ipeim.rnu.tn (K. Bouzouita).

1631-0748/$ – see front matter © 2011 Académie des sciences. Published by Elsevier Masson SAS. All rights reserved.
doi:10.1016/j.crci.2011.04.005

Several processes have been developed for the preparation of britholites. Usually, they are obtained via a solid state reaction at high temperature [3–5,17,18]. Therefore, it seems interesting to attempt the preparation of these britholites by a mechanochemical synthesis.

The mechanochemical synthesis was originally developed by Benjamin and co-workers in the early 1970s to obtain metallic compounds whose elaboration with the conventional methods is often ineffective [19]. Since the 1980s, the works of Yermakov et al. [20] and Koch et al. [21] have permitted to extend the use of this method for the preparation of a wide range of materials.

In the mechanochemical synthesis, a mixture of elementary powders is submitted in a mill to intense successive shocks with adjustable frequencies and energies. These shocks by creating punctual, linear or surface defects induce an increase in the free energy of the initial material. Therefore, to minimize the free energy, change and transformation phases occur in the system leading to the desired product [22,23]. Thus, this method, which involves only a solid-state reaction at room temperature, seems quite appealing. Indeed, besides its simplicity, speed and low power consumption, it is a valuable method for industrial production. Moreover, it allows one to obtain powders with a large specific surface area, permitting a lowering in the sintering temperatures [24–26].

In this work, we attempt to prepare fluorbritholites with the chemical formula of $Sr_{10-x}La_x(PO_4)_{6-x}(SiO_4)_xF_2$ with $0 \le x \le 6$, by a mechanochemical synthesis. In the following sections, the samples will be assigned as $Sr_{10-x}La_x$ where x designs the used La content.

The phase evolution with milling duration was followed by using the X-ray diffraction (XRD) and infrared spectroscopy (IR).

2. Experimental procedure

2.1. Powders preparation

The starting materials were of an analytical grade: strontium carbonate ($SrCO_3$) (> 96% Riedel de Haen), lanthanum oxide (La_2O_3) (> 99.5% Prolabo), silica (SiO_2) (> 99.5% Alfa), strontium fluoride (SrF_2) (> 99.5% Prolabo), and strontium diphosphate ($Sr_2P_2O_7$).

2.1.1. Preparation of $Sr_2P_2O_7$

The strontium diphosphate was prepared by using the solid state reaction at 900 °C for 10 h, according to the following equation:

$$2SrCO_3 + 2(NH_4)_2HPO_4 \rightarrow Sr_2P_2O_7 + 4NH_3(\uparrow) + 2CO_2(\uparrow) + 3H_2O(\uparrow) \quad (1)$$

2.1.2. Preparation of britholites

Britholites with the chemical formula of $Sr_{10-x}La_x(PO_4)_{6-x}(SiO_4)_xF_2$ with $0 \le x \le 6$ were prepared according to the following equation:

$$SrF_2 + 3SrCO_3 + (6-x)/2Sr_2P_2O_7 + x/2La_2O_3 + xSiO_2 \rightarrow Sr_{10-x}La_x(PO_4)_{6-x}(SiO_4)_xF_2 + 3CO_2(\uparrow) \quad (2)$$

Before use, the lanthanum oxide was calcined at 1000 °C for 2 h. Indeed, when light rare earth oxides are exposed to air, there is formation of the corresponding hydroxides [27].

The mechanochemical synthesis was performed in a Fritsch Pulverisette 7 planetary micro mill using stainless steel balls with a diameter of 12 mm and a stainless steel cell of 45 cm^3. The cell was loaded with several balls and raw materials at appropriate amounts to obtain stoichiometric apatites as given in the Eq. (2). The mass of the powder was 1 g and the balls-to-powder mass ratio was 34:1. The rotating disc speed and cell speed were 500 and 1000 rpm, respectively. The experimental conditions were a shock kinetic energy of 0.151 J/shock, a shock frequency of 100 Hz and an injected power shock of 15.1 Watt/g. The milling was carried out without any additives for different durations, and the powders were heat-treated under an argon flow at 900 and 1100 °C for 12 h with a heating rate of 10 °C/min.

2.2. Powder characterization

XRD patterns of both as-milled and heat-treated powders were carried out on an X'Pert Pro, PANalytical diffractometer using Cu Kα radiation. Scans were run from 20 to 65° (2θ) with a step size of 0.03°, and a counting time of 1 s per step. The experimental patterns were compared to standards compiled by the Joint Committee on Powder Diffraction and Standards (JCPDS) using the X'Pert HighScore Plus software. The lattice parameters of both as-prepared and heat-treated samples were determined by Rietveld refinement of the XRD data using the Fullprof program [28]. The refinements were based on the structural data of the JCPDS card No. 00-050-1744 using the space group $P6_3/m$.

Infrared spectra were recorded in the range of 4000–400 cm^{-1} with an EQUINOX 55 TF-IR spectrometer equipped with OPUS/IR software, and a PerkinElmer Spectrum 100 spectrometer, using the KBr pellets technique.

3. Results

3.1. X-ray diffraction

As can be observed from Fig. 1, after 5 h of milling, the XRD patterns show reflections of a dominant apatite phase indexed in the hexagonal system (space group $P6_3/m$) based on the strontium fluorapatite pattern (JCPDS #00-050-1744). The other reflections correspond to the starting materials, identified by their reflections: SiO_2, at 20.85° (JCPDS #01-085-0798), La_2O_3, at 52.49° (JCPDS #01-074-2430) and $SrCO_3$, at 44.38° (JCPDS #01-074-1491). The two latter reagents were only observed for $x \ge 5$, while silica was detected from $x = 2$. Nevertheless, the presence of other reactants and/or intermediate phases could not be excluded. They were not detected probably due to their low amounts or because they were in an amorphous phase. If we assume – in agreement with the XRD patterns – that all the reagents had reacted, it seems possible to obtain in a

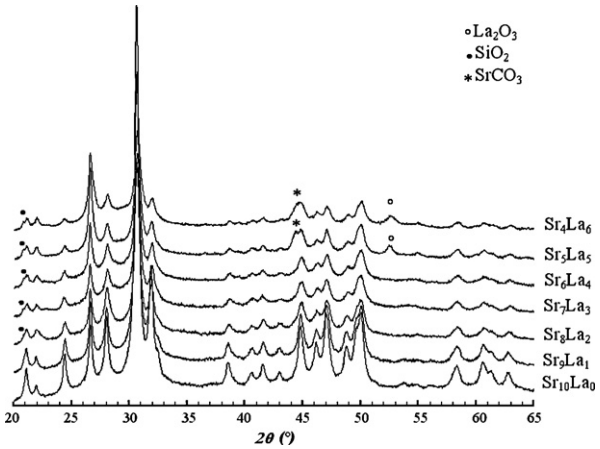

Fig. 1. XRD patterns of all the samples milled for 5 h.

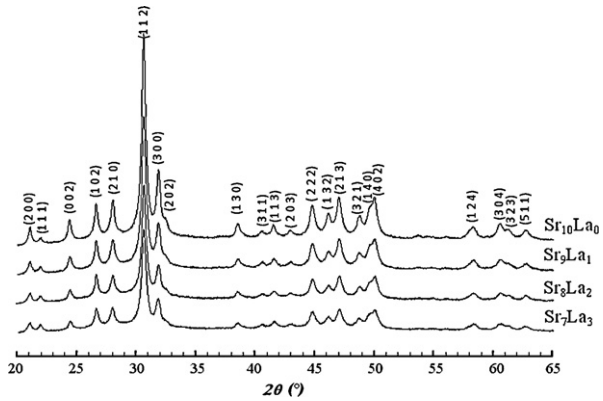

Fig. 3. XRD patterns of samples with $x \leq 3$ milled for 20 h.

pure state the monosubstituted britholite and obviously the pure fluorapatite by a simple milling for 5 h. However, for the compositions richer in Si, a prolonged milling over 5 h is required.

Previous studies have demonstrated that the formation enthalpy of the series of Ca-La-fluorbritholites ($Ca_{10-x}La_x(PO_4)_{6-x}(SiO_4)_xF_2$, with $0 \leq x \leq 6$) increased when the incorporated amounts of lanthanum and silicate rose [29]. Furthermore, it was shown that the monosilicate britholite is not affected by the metamictisation due to the alpha particles and recoil nuclei, despite the intense internal and external irradiation doses [15,16]. Thus, a selected composition, $Sr_8La_2(PO_4)_4(SiO_4)_2F_2$ was chosen to conduct a more detailed study. Indeed, if this compound is obtained in a pure state, the preparation of the monosubstituted sample is therefore possible.

Fig. 2 shows the XRD patterns of the Sr_8La_2 sample milled between 0.5 and 20 h. From these patterns, we notice that for 0.5 h of milling, practically all the peaks belong to the reagents. Nonetheless, one can see the emergence of peaks as shoulders located at 2θ angles of 21.97°, 24.42° and 31.87°, indicating a beginning of the formation of an apatite phase. As the milling process progressed, the intensities of the peaks of the starting materials gradually decreased and those of the apatite peaks increased. All the reactants disappeared for a milling duration higher than 1 h, except La_2O_3 and SiO_2. If La_2O_3 disappeared for a milling duration higher than 3 h, SiO_2 remained present for up to 10 h. After milling for 15 and 20 h, XRD pattern show the peaks corresponding only to britholites, and no other phases such as La_2O_3 and SiO_2 were detected.

Figs. 3 and 4 give the XRD patterns of samples with $0 \leq x \leq 6$, milled for 20 h. For $x \leq 3$, The XRD patterns showed only the peaks belonging to the apatite (Fig. 3), while for $x > 3$, the XRD patterns contained in addition to the peaks of the britholite those of SiO_2, the intensities of these latter increased as x increased (Fig. 4). As not all SiO_2 was incorporated into the apatite structure, according to Eq. (2), a certain amount of La_20_3 would also remain in the powder after reaction.

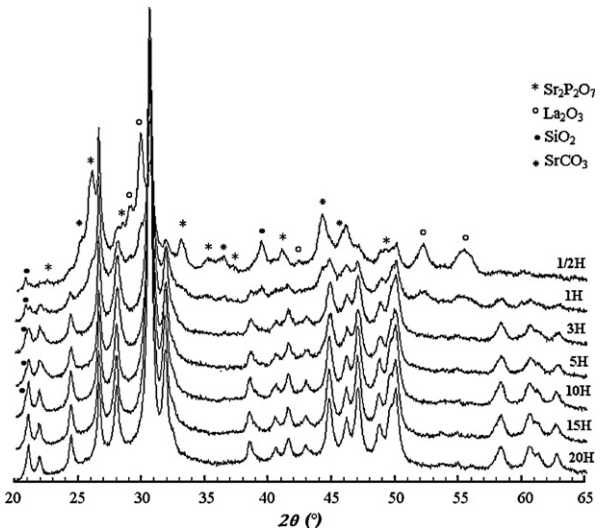

Fig. 2. XRD patterns of the Sr_8La_2 sample milled between 0.5 and 20 h.

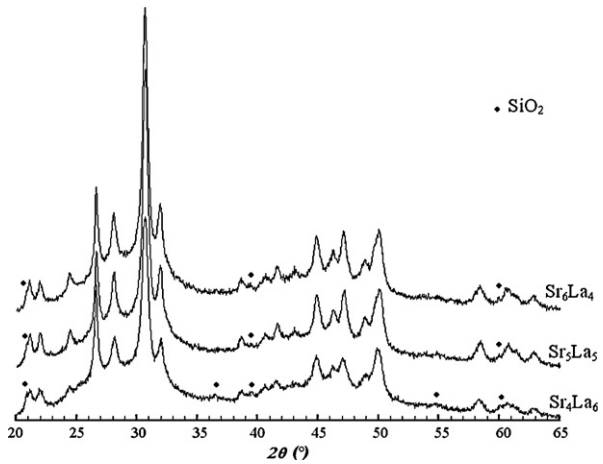

Fig. 4. XRD patterns of samples with $4 \leq x \leq 6$ milled for 20 h.

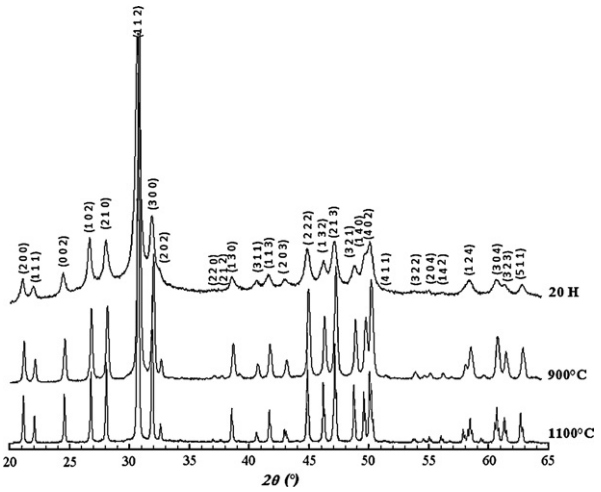

Fig. 5. XRD patterns of the Sr_8La_2 sample heat-treated at 900 and 1100 °C after milling for 20 h.

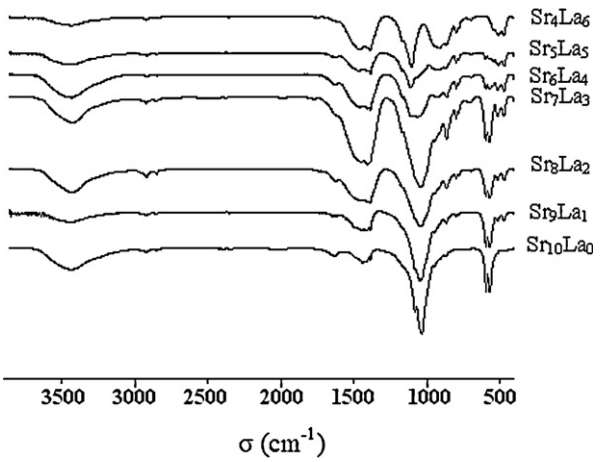

Fig. 6. FTIR spectra of all the samples milled at 5 h.

Fig. 5 shows the XRD patterns of the Sr_8La_2 sample heat treated at 900 and 1100 °C for 12 h after milling for 20 h. As can be noticed, the patterns presented only the peaks of the apatite and no peaks corresponding to other compounds could be detected.

3.2. Infrared spectroscopy

The IR absorption spectra of the samples obtained after 5 h of milling are shown in Fig. 6. These spectra continuously changed with the increase of the amount of silicate used. The attribution of the bands associated PO_4 and SiO_4 groups were carried out by comparison with the spectra of apatite phases with similar compositions, reported in the literature [4–7,9,30–32].

For the nonsubstituted sample, the spectrum exhibited the characteristic bands of PO_4^{3-} ions at 1080–1034 cm^{-1} attributed to the asymmetric stretching modes P-O (ν_3), 948 cm^{-1} associated to the symmetric stretching mode P-O-P (ν_1), 567 and 592 cm^{-1} assigned to asymmetric bending modes O-P-O (ν_4). Besides, there are some additional bands. The strong doublet appearing at 1438 and 1417 cm^{-1} and the band at about 866 cm^{-1} were attributed to the stretching vibrations and deformation vibrations, respectively, of the C-O bonds in the CO_3^{2-} anions, which were located in the PO_4^{3-} sites (B-type substitution) [33,34]. The high intensities of these latter bands indicate that a significant proportion of carbonates resulting from the raw materials were incorporated into the apatite phase. The bands appearing at 3441 and

Table 1
Assignment of the IR absorption bands for the $Sr_{10-x}La_x(PO_4)_{6-x}(SiO_4)_xF_2$ samples milled for 5 h.

Composition	PO_4^{3-}			SiO_4^{4-}		
	ν_1(cm^{-1})	ν_3(cm^{-1})	ν_4(cm^{-1})	ν_1(cm^{-1})	ν_3(cm^{-1})	ν_4(cm^{-1})
$Sr_{10}(PO_4)_6F_2$	948	1034 1080	592 567	-	-	-
$Sr_9La(PO_4)_5(SiO_4)F_2$	946	1044 1080	593 567	866	915	513 469
$Sr_8La_2(PO_4)_4(SiO_4)_2F_2$	943	1041 1083	593 566	863	915	512 467
$Sr_7La_3(PO_4)_3(SiO_4)_3F_2$	945	1042 1081	593 567	862	916	512 469
$Sr_6La_4(PO_4)_2(SiO_4)_4F_2$	942	1058	595 569	863	917 1103	546 511 468
$Sr_5La_5(PO_4)(SiO_4)_5F_2$	939	1061	594 569	870	915 1110	544 511 469
$Sr_4La_6(SiO_4)_6F_2$	-	-	-	869	917 1103	543 508 471

1634 cm^{-1} correspond to the adsorbed water on the particle's surface.

As far as the substituted samples are concerned, the FTIR spectra showed significant changes compared with the pure apatite. Besides those corresponding to PO_4^{3-}, and obviously to CO_3^{2-} groups, additional bands were detected. For $x = 1$, the bands at 469 and 513 cm^{-1} could be assigned to the SiO_4^{4-} groups [35], while the bands observed at 799, 778 and 690 cm^{-1} were ascribed to SiO_2 [36,37]. This latter compound was not detected by the XRD analysis because of its low amount or its presence in the amorphous or nanocrystallized forms. With the increase in the substituent amounts, we notice a decrease in the intensities of PO_4 groups' bands and an increase of those of SiO_4. The bands' frequencies associated with these two latter groups for the different compositions are presented in Table 1.

The IR absorption spectra for the Sr_8La_2 sample milled between 0.5 and 20 h are given in Fig. 7. These spectra clearly show the progression of the formation of the apatite phase. However, the complexity of the system due to the many used reagents made the assignment of the observed bands difficult. After 3 h of milling (Fig. 7(a)), the spectrum exhibited the vibration bands of an apatite phase and the disappearance of the vibration bands corresponding to the raw materials. In comparison with the spectrum of the sample milled for 0.5 h, we noticed the disappearance of bands positioned at 469, 486, 501, 546, 704, 747, 778, 799, 860, 980, 1013, 1106, 1142, 1385 and 1461 cm^{-1} which correspond to reactants. The bands appearing at 1047, 947, 592 and 563 cm^{-1} were assigned to PO_4 groups, while the band centered at 512 cm^{-1} was assigned to O-Si-O asymmetric bending ν_2 in the SiO_4 groups [35]. This latter band serves as an evidence for the incorporation of SiO_4 groups into the apatite structure. The bands appearing at 1469 and 1408 cm^{-1} were unambiguously attributed to carbonate groups. When the powder was subjected to a longer milling duration, the spectra still remained practically identical. We notice that the characteristic bands of the carbonate rmained present even after 20 h of milling (Fig. 7(b)).

The IR spectra of the Sr_8La_2 sample heat-treated at 900 and 1100 °C after milling for 20 h are shown in Fig. 8. As observed, the heat treatment caused a significant change. The absorption bands became sharp and intense. Furthermore, at 900 °C, a decrease in intensities of peaks associated to the carbonate groups and SiO_2, and concomitantly an increase in the intensities of the bands due to SiO_4 groups were observed. At 1100 °C, the doublet at 1407 and 1443 cm^{-1} was absent, follows the removal of CO_2 gas. Also, we noticed the disappearance of the characteristic bands associated to SiO_2, observed previously for the milled powder such as the bands at 799, 778 and 690 cm^{-1}. This indicates the formation of a pure apatitic powder. Thus, typical absorption bands of PO_4^{3-} vibrations ν_1, ν_3 and ν_4 were observed at 946, 1080–1040 and 593–568 cm^{-1}, respectively. However, the fundamental vibrational modes of SiO_4^{4-} groups in an apatitic environment are witnessed in the region around 918 cm^{-1} (ν_3), 866–840 cm^{-1} (ν_1) and at 544–507 cm^{-1} (ν_4). In addition, the band positioned at about 866 cm^{-1}, which was attributed to the CO_3^{2-} groups for the milled powder, has dramatically decreased in intensity after heat-treatment and departure of CO_2, but it was still present after heat treatement. Therefore, it was also assigned to SiO_4^{4-} groups [35].

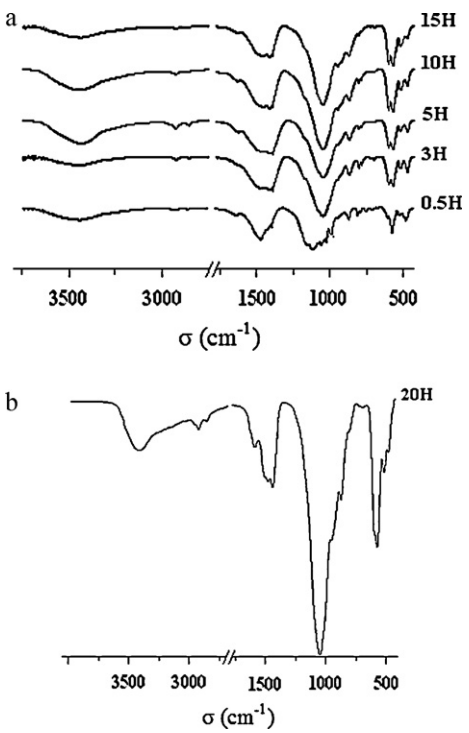

Fig. 7. FTIR spectra of the Sr_8La_2 sample milled between 0.5 and 15 h; (b) for 20 h.

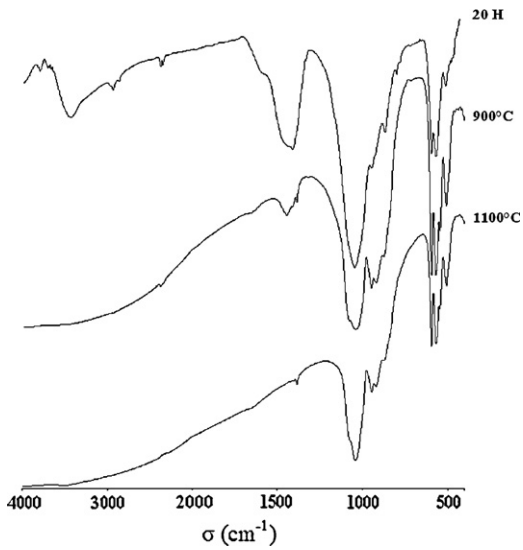

Fig. 8. FTIR spectra of the Sr_8La_2 sample milled at 20 h and calcined at 900 and 1100 °C.

Table 2
lattice parameters of the Sr_8La_2 sample heat-treated at 900 and 1100 °C after milling for 20 h.

	Sr_8La_2		
	a(Å)	c(Å)	V(Å^3)
As-milled	9,708(3)	7,265(2)	593,04(4)
Heat-treated at 900 °C	9,713(2)	7,267(4)	593,77(3)
Heat-treated at 1100 °C	9,740(4)	7,272(1)	597,47(2)

3.3. Lattice parameters

The lattice parameters for both as-prepared and heat-treated Sr_8La_2 sample determined by Rietveld refinement of the XRD data using the Fulprof program are presented in Table 2. For the as-prepared sample, the parameters are quite different from those of the same composition obtained by the solid state reaction at high temperature, $a = 9.727(1)$ Å and $c = 7.277(2)$ Å [18]. This result can be explained by the substitution of PO_4^{3-} ions (the average lengths of P-O is 1.51 Å) by both more and less voluminous ions, SiO_4^{4-} (the average lengths of Si-O is 1.62 Å) [38] and CO_3^{2-} (the average lengths of C-O is 1.25 Å) [38], respectively, on the one hand, and the creation of vacancies in the Sr-sites following the substitution of PO_4^{3-} ions by CO_3^{2-} ones, on the other hand. It is worth noting that the charge balance following the substitution of PO_4^{3-} ions by SiO_4^{4-} ones is performed by the substitution of La^{3+} ions for Sr^{2+} ones. The sum of these effects results in a decrease of the lattice parameters, with respect to the sample obtained at a high temperature.

When the powder was heat-treated at 1100 °C, the obtained results have indicated that the powder was formed by a pure apatite phase, and no secondary phases were detected. The Rietveld analysis has shown an increase in the lattice parameters, with respect to the as-prepared sample (Table 2). These values agree with those obtained in ref. [18]. These changes in the lattice parameters resulted from the elimination of the carbonates, as it will be shown below, and the incorporation of SiO_2 and La_2O_3, which were not inserted into the apatite structure during the milling.

4. Discussion

4.1. As-prepared powder

For the synthesis, the amount of reactants was calculated by assuming that the silicate ions substituted the phosphate ions, according to the Eq. (2). During milling, the decrease of the diffraction peaks of SiO_2 and La_2O_3 served as evidence that SiO_4^{4-} and La^{3+} entered into the apatite lattice, especially since any other compound containing the latter species was detected even after heat treatment, as it will be show below. However, the IR spectroscopic analysis showed that all the used SiO_2 amount was not completely consumed by the synthesis reaction during the milling. Furthermore, this technique revealed that some carbonate ions were inserted into the apatite's lattice in the B-site. Thus, both anionic ions, SiO_4^{4-} and CO_3^{2-}, were substituted for PO_4^{3-} into the apatite's framework. This substitution can be written as follows [39]:

$$(PO_4)_{6-x}(SiO_4)_y(CO_3)_u \tag{3}$$

where $x = y + u$

One has to bear in mind that the B-sites must be fully occupied, i.e., the total number of the anionic groups must be equal to six and at most u is equal to 3, according to Eq. (2). In these conditions, an amount of SiO_2, equivalent to that of the incorporated carbonate into the apatite framework, must remain in the milled powder in its original form or in a secondary phase. According to the XRD analysis, SiO_2 was remained in the powder after milling.

Depending on the incorporated carbonate amount, two cases can be observed:

(i) The incorporated amounts of SiO_4^{4-} and CO_3^{2-} are equal ($y = u$ and $x = 2y$). So, there is a mutual charge balance. Using Kröger-Vink notation, this can be written as follows:

$$2y\,PO_4^{\times}{}_{PO4} = y\,CO_3^{\circ}{}_{PO4} + y\,SiO_4^{'}{}_{PO4} \tag{4}$$

Nonetheless, the substitution of La^{3+} for Sr^{2+} implies the creation of cationic vacancies to compensate for the electric neutrality. If we assume that all the introduced strontium has participated in the reaction, the cationic vacancies were created according to the following mechanism:

$$2y\,Sr^{\times} = 4y/3\,La^{\circ} + 2y/3\,V''_{Sr} \tag{5}$$

where V_{sr} stands for a vacancy in the Sr-sublattice. This equation supposed that all the La^{3+} ions, initially used, were not completely incorporated into the apatite lattice.

Considering the electric neutrality requirement, the global substitution mechanism is given by:

$$2y\,Sr^{\times} + 2y\,PO_4^{\times}{}_{PO4} = y\,CO_3^{\circ}{}_{PO4} + y\,SiO_4^{'}{}_{PO4} + 4y/3\,La^{\circ} + 2y/3\,V''_{Sr} \tag{6}$$

The corresponding generic formula is:

$$Sr_{10-2y}La_{4y/3}V_{2y/3}(PO_4)_{6-2y}(SiO_4)_y(CO_3)_yF_2 \tag{7}$$

According to the above mechanism, y mol of SiO_2 and $y/3$ mol of La_2O_3 remained in the mixture in their original form or in a secondary phase. As mentioned previously, the characterization results showed that no secondary phase was formed, but a certain amount of SiO_2 remained in the powder after milling. In these conditions, La_2O_3 must also be found in the powder. It was not detected by XRD probably because of its very low amount.

(ii) The incorporated amounts of SiO_4^{4-} and CO_3^{2-} were different. Two cases can be distinguished:

$-y > u$, i.e., an excess of silicate ($w = y - u$ and $x = 2u + w$), with respect to the carbonate, was incorporated into the apatite. The resulting negative charge excess (w) is compensated by an equivalent number of La^{3+} ions, according to the following equation:

$$w\,Sr^{\times} + w\,PO_4^{\times}{}_{PO4} = w\,La^{\circ} + w\,SiO_4^{'}{}_{PO4} \tag{8}$$

Taking into account the Eqs. (6), (7) and (8), the global substitution mechanism is given by:

$$(2u+w)PO_4^{\times}{}_{PO4} + (2u+w)_{Sr}{}^{\times}{}_{Sr} = (u+w)SiO_4^{'}{}_{PO4} + u\,CO_3^{\circ}{}_{PO4} + (4u+3w)/3\,La^{\circ} + 2u/3\,V''_{Sr} \quad (9)$$

The corresponding generic formula may be written as follows:

$$Sr_{10-(2u+w)}La_{(4u+3w)/3}V_{2u/3}(PO_4)_{6-(2u+w)}(SiO_4)_{(u+w)}(CO_3)_uF_2 \quad (10)$$

In this case, the quantities of SiO_2 and La_2O_3 not incorporated into the apatite correspond to u mol and $u/3$ mol, respectively.

$y < u$, i.e., the number of the incorporated carbonate ions (u) was higher than that of the silicate ions (y). The excess of the carbonate ions is given by: $z = u - y$ and $x = 2y + z$.

In these conditions, following the substitution of SiO_4^{4-} and CO_3^{2-} for PO_4^{3-}, the charge compensation occurred by the creation of vacancies in the Sr-sublattice, according to the following equation:

$$(2y+z)PO_4^{\times}{}_{PO4} = y\,SiO_4^{'}{}_{PO4} + (y+z)CO_3^{\circ}{}_{PO4} + z/2\,V''_{Sr} \quad (11)$$

Disregarding this latter equation, and considering the electrical neutrality, the substitution of La^{3+} for Sr^{2+} can be formulated as:

$$(2y+z)_{Sr}{}^{\times}{}_{Sr} = (4y+2z)/3\,La^{\circ} + (2y+z)/3\,V''_{Sr} \quad (12)$$

Finally, the global mechanism can be described as follows:

$$(2y+z)Sr^{\times} + (2y+z)PO_4{\times}_{PO4} = y\,SiO_4^{'}{}_{PO4} + (y+z)CO_3^{\circ}{}_{PO4} + (8y+z)/6\,La^{\circ} + (4y+5z)/6\,V''_{Sr} \quad (13)$$

and the corresponding generic formula as:

$$Sr_{10-(2y+z)}La_{(8y+z)/6}V_{(4y+5z)/6}(PO_4)_{6-(2y+z)}(SiO_4)_y(CO_3)_{(y+z)}F_2 \quad (14)$$

The quantities of SiO_2 and La_2O_3 not incorporated into the apatite correspond to $(y+z)$ (i.e. u) and $(4y+5z)/12$ (i.e. $(5u-y)/12$) mol, respectively.

4.2. Powders' calcination

The calcination did not appear to significantly affect the XRD patterns except for a narrowing of the peaks, indicating a higher crystallinity of the powder. Furthermore, no secondary phases could be detected other than the apatite. However, the IR spectra significantly changed after calcination at 1100 °C. No bands corresponding to the carbonate groups were detected and there was an increase in the intensities of the bands associated with the SiO_4^{4-} groups. As no secondary phases were formed after calcination, the pure apatite could result from the reaction between the carbonated apatite and the SiO_2 and La_2O_3 amounts remaining in the powders, following three equations, depending on the incorporated silicate and carbonate amounts:

In the case where the incorporated SiO_2 and La_2O_3 had an identical molar number, the reaction leading to the pure britholite might be written as follows:

$$Sr_{10-2y}La_{4y/3}V_{2y/3}(PO_4)_{6-2y}(SiO_4)_y(CO_3)_yF_2 + y\,SiO_2 + y/3\,La_2O_3 \rightarrow Sr_{10-2y}La_{2y}(PO_4)_{6-2y}(SiO_4)_{2y}F_2 + y\,CO_2(\uparrow) \quad (15)$$

and the corresponding mechanism can be described as:

$$y\,CO_3^{\circ}{}_{PO4} + 2y/3\,V''_{Sr} + y\,SiO_2 + y/3\,La_2O_3 = y\,SiO_4^{'}{}_{PO4} + 2y/3\,La^{\circ} + y\,CO_2 \quad (16)$$

However, when the molar numbers of SiO_4^{4-} and CO_3^{2-} are different ($y \neq u$), the two following cases must be considered:

For $y > u$, the following reaction would occur:

$$Sr_{10-(2u+w)}La_{(4u+3w)/3}V_{2u/3}(PO_4)_{6-(2u+w)}(SiO_4)_{(u+w)}(CO_3)_uF_2 + uSiO_2 + u/3\,La_2O_3 \rightarrow Sr_{10-(2u+w)}La_{(2u+w)}(PO_4)_{6-(2u+w)}(SiO_4)_{(2u+w)}F_2 + u\,CO_2(\uparrow) \quad (17)$$

and the mechanism leading to the formation of the pure britholite can be written as:

$$u\,CO_3^{\circ}{}_{PO4} + 2u/3\,V''_{Sr} + u\,SiO_2 + u/3\,La_2O_3 = u\,SiO_4^{'}{}_{PO4} + 2u/3\,La^{\circ} + u\,CO_2 \quad (18)$$

For $y < u$, the reaction leading to the pure britholite is:

$$Sr_{10-(2y+z)}La_{(8y+z)/6}V_{(4y+5z)/6}(PO_4)_{6-(2y+z)}(SiO_4)_y(CO_3)_{(y+z)}F_2 + (y+z)SiO_2 + (4y+5z)/12\,La_2O_3 \rightarrow Sr_{10-(2y+z)}La_{(2y+z)}(PO_4)_{6-(2y+z)}(SiO_4)_{(2y+z)}F_2 + u\,CO_2(\uparrow) \quad (19)$$

The corresponding mechanism can be formulated as:

$$(y+z)CO_3^{\circ}{}_{PO4} + (4y+5z)/6\,V''_{Sr} + (y+z)SiO_2 + (4y+5z)/12La_2O_3 = (y+z)SiO_4^{'}{}_{PO4} + (4y+5z)/6La^{\circ} + (y+z)CO_2 \quad (20)$$

The IR spectroscopy, has revealed the presence of strong absorption bands associated to the carbonates. Nonetheless, for the powders milling for 5 h, although the IR spectra have shown that the intensities of the bands attributed to carbonates decreased when the milling progressed, it seems that the incorporated amount of this species was higher than that of silicates. In these conditions, the mechanism leading to the formation of carbonated britholites and pure britholites during calcination would correspond to Eq. (13) and Eq. (20), respectively.

5. Conclusion

In this study, we attempted to prepare strontium fluorbritholites with the chemical formula $Sr_{10-x}La_x(PO_4)_{6-x}(SiO_4)_xF_2$ (where $0 \leq x \leq 6$) from SrF_2, $SrCO_3$, $Sr_2P_2O_7$, La_2O_3 and SiO_2 by the mechanochemical synthe-

sis. The X-ray diffraction and FTIR spectroscopy identified the resultant powders as carbonated britholites. An amount of silica equivalent to that of the incorporated carbonates and some amount of lanthanum oxide remained in the powders after milling. The obtaining of pure britholites needed a heat-treatment at 1100 °C. The mechanism leading to the formation of the pure britholites was also discussed. The obtained results suggest that the use of raw materials containing no carbonate should lead, by a suitable grinding at room temperature, to pure britholites.

Acknowledgements

The authors would like to thank F.H. Ayedi for his useful discussions, and A. Hadroug for his help with English.

References

[1] R. Bodu, H. Bouzigues, N. Morin, J.P. Pfiffelmann, C. R. Acad. Sci. Ser 275 (1972) 1731.
[2] V. Sère, Des minéraux néoformés à Oklo (Gabon), histoire géologique du bassin d'Oklo : une contribution pour les études de stockages géologiques de déchets radioactifs, PhD Thesis, University of Paris 7, 1996.
[3] N. Dacheux, N. Clavier, A. Robisson, O. Terra, F. Audubert, J. Lartigue, C. Guy, C. R. Chimie 7 (2004) 1141.
[4] O. Terra, N. Dacheux, F. Audubert, R. Podor, J. Nucl. Mater 352 (2006) 224.
[5] O. Terra, F. Audubert, N. Dacheux, C. Guy, R. Podor, J. Nucl. Mater 354 (2006) 49.
[6] O. Terra, F. Audubert, N. Dacheux, C. Guy, R. Podor, J. Nucl. Mater 366 (2007) 70.
[7] E. Du Fou de Kerdaniel, N. Clavier, N. Dacheux, O. Terra, R. Podor, J. Nucl. Mater 362 (2007) 451.
[8] E. Veilly, E. du Fou de Kerdaniel, J. Roques, N. Dacheux, N. Clavier, Inorg. Chem 47 (2008) 10971.
[9] N. Dacheux, E. Du Fou De Kerdaniel, N. Clavier, R. Podor, J. Aupiais, et al. J. Nucl. Mater 404 (2010) 33.
[10] D.K. Bhattacharyya, App. Rad. and Iso 49 (1998) 215.
[11] G.R. Lumpkin, K.L. Smith, M.G. Blackford, K.P. Hart, P. McGlinn, R. Giere, C.T. Williams, Transactions of the American Nuclear Society 70 (suppl. 1) (1994) 879.
[12] G.R. Lumpkin, K.L. Smith, M.G. Blackford, R. Giere, C.T. Williams, Mater. Res. Soc. Sym. Proc 412 (1996) 329.
[13] G.R. Lumpkin, Nuc. Mater 289 (2001) 136.
[14] C.T. Williams, R. Giere, Bulletin of the Natural History Museum (London (Geol.)) 52 (1996) 1.
[15] J. Chaumont, S. Soulet, J.C. Krupa, J. Carpena, Nuc. Mater 301 (2–3) (2002) 122.
[16] S. Soulet, J. Carpena, J. Chaumont, O. Kaitasov, M.O. Ruault, J.C. Krupa, Nuclear Instruments & Methods in Physics Research, Section B (Beam Interactions with Materials-and Atoms) 184 (3) (2001) 383.
[17] R. El Ouenzerfi, G. Penczer, C. Goutaudier, M.T. Cohen-Adad, G. Boulon, M. Trabelsi Ayadi, N. Kbir-Ariguib, Opt. Mater 16 (2001) 301.
[18] K. Boughzala, E. Ben Salem, A. Ben Chrifa, E. Gaudin, K. Bouzouita, Mater. Res. Bull 42 (2007) 1221.
[19] J.S. Benjamin, Metall. Trans 1 (1970) 2943.
[20] A.E. Yermakov, E.E. Yurchikov, V.A. Barinov, Phys. Met. Metall 52 (1981) 8.
[21] C.C. Koch, O.B. Cavin, C.G. Mekamey, J.O. Scarbrough, Appl. Phys. Lett 43 (11) (1983) 1017.
[22] M. Abdellaoui, E. Gaffet, Acta. Metall. Mater 43 (1995) 1087.
[23] M. Abdellaoui, E. Gaffet, J. Alloys Compd 209 (1994) 351.
[24] J. Meng, C.C. Jia, Q. He, Powder metallurgy 51 (2008) 227.
[25] J. Sun, M. Wang, X. Li, Z. He, Y. Zhao, Key Engineering Materials 353–358 (2007) 1350.
[26] K.A. Khor, Y. Li, Materials science and engineering 256 (1998) 271.
[27] T. Kharlamova, S. Pavlova, V. Sadykov, O. Lapina, D. Khabibulin, T. Krieger, V. Zaikovskii, A. Ishchenko, A. Salanov, V. Muzykantov, N. Mezentseva, M. Chaikina, N. Uvarov, J. Frade, C. Argirusis, J. Solid State Ionics 179 (2008) 1018.
[28] J. Rodriguez-Carvajal, FULLPROF: a program for Rietveld refinement and pattern matching analysis, in: Collected Abstract of Powder Diffraction Meeting, Toulouse, France, 1990, pp. 127.
[29] K. Ardhaoui, M.V. Coulet, A. Ben Chrifa, J. Caperna, J. Rogez, M. Jemal, Thermochim. Acta 444 (2006) 190.
[30] S. Khorari, R. Cahay, A. Rulmont, Eur. J. Solid State Inorg. Chem 31 (1994) 921.
[31] B.O. Fowler, Inorg. Chem 13 (1974) 194.
[32] J. Neubauer, H. Pollmann, N. Jahrb, Mineral. Abd 168 (1995) 58.
[33] H.E. Feki, J.M. Savariault, A. Ben Salah, J. Alloys Compd 287 (1999) 114.
[34] J.P. Lafon, E. Champion, D. Bernache-Assollant, J. Eur. Ceram. Soc 28 (2008) 139.
[35] E. Rodriguez-Reyna, A.F. Fuentes, M. Maczka, J. Hanuza, K. Boulahya, U. Amador, J. Solid State Chem. 179 (2006) 522.
[36] G. Tzvetkov, N. Minkova, Mater. Lett 39 (1999) 354.
[37] M. Hadioui, Synthèse d'hydroxyapatite et de silices greffées pour l'élimination de métaux toxiques en solution aqueuse, PhD Thesis, University of Toulouse III, France, 2007.
[38] R.D. Shannon, Acta Crystallogr. A 32 (1976) 751.
[39] M. Palard, E. Champion, S. Foucaud, J. Solid State Chem. 181 (2008) 1950.